

INTEGRITY MONITORING OF TIGHTLY INTEGRATED BDS/SINS USING MULTI-HYPOTHESIS SOLUTION SEPARATION (MHSS) ALGORITHM

Shuguang SUN¹, Haolin WANG¹, Ruihua LIU¹, Shan KUANG², Wantong CHEN¹

¹Civil aviation university of China, Tianjin, China ² Lingfeng aviation R&D Center, Shenzhen, China

Abstract

Tightly integrated BDS/SINS (BeiDou Navigation Satellite System/Strap-down Inertial Navigation System) navigation system provides higher accuracy performance with the continuously calibration of the inertial measurement units (IMUs)' errors using satellite measurements and better continuity performance profited from SINS aiding under poor satellites coverage, which is appreciated in aircraft performance based navigation (PBN) operation. But tightly integration also means that the system can propagate the established position even if the satellite signals are lost or unexpected satellite failure occurs, which will cause integrity risk because of the mis-calibration due to the undetected failure. This paper explores the MHSS (multi-hypothesis solution separation) algorithm in tightly integrated BDS/SINS system for integrity monitoring, multiple Kalman filters provide a non-transient detection capability to enhance its integrity monitoring function based on inertial redundancy information retained from previously processed measurements. BDS satellites information from BDS ground station and simulated aircraft flight trajectory are used to verify the integrity monitoring algorithm by intentionally added errors to the satellites pseudo-range. Monte Carlo simulation techniques is introduced to verify its FDE (fault detection and exclusion) performance, calculated horizontal protection level (HPL) is compared with system horizontal error. The simulation results show that the BDS/SINS tightly integrated navigation system based on multi-hypothesis solution separation algorithm can detect and identify the faulted satellite effectively, and the calculated horizontal protection level (HPL) is in line with expectations.

Keywords: Tightly integrated BDS/SINS, Integrity monitoring, MHSS, Kalman-filter

1. Introduction

Integrity is a safety-critical requirement of civil aviation PBN operation which makes the airborne navigation system to provide timely and valid warnings to the user (alerts) when the system must not be used for the intended operation (or phase of flight). There are two main objectives of navigation system integrity monitoring function: one is fault detection and exclusion (FDE) of faulty navigation measurements, the other is horizontal protection level (HPL) calculation. Fault detection and exclusion use redundant measurements information to ensure the navigation calculation won't be polluted by the faulted satellite, and HPL is computed to ensure the pilots be warned in time when the navigation outputs go beyond the performance of service of interest (Horizontal Alert (HAL) Limits of 556 m and 185 m, corresponding to the RNP0.1 and RNP0.3 operations). Most available FDE algorithms are detect and isolate faulted satellite in two distinct steps with a linear unbiased estimator, such as a least squares filter, or an estimator that merges the fault detection and exclusion functions [1~5]. These approaches work very well in many applications and is the basis for the standard approaches in RAIM and Advanced RAIM (A-RAIM) especially for un-augmented GNSS.

For airborne based augmentation system such as tightly integrated BDS/SINS system, as the position update rate lower than the SINS output, the growth in the solution error between updates must be considered, which means integrity coasting should be considered. Integrity coasting is the propagation of the position and corresponding integrity bound assuming the worst case satellite undetected failure was in progress just prior to the loss of BDS satellite, the HPL computation must take into account the mis-calibration of the hybrid solution due to the undetected failure in order to provide high and accurate integrity error bounds in the presence of faulty measurements [6]. MHSS fault detection and exclusion mechanism is chosen to implement the integrity monitoring with inertial propagated geometric redundancy in BDS/SINS integration.

According to RTCA DO-316(minimum operational performance standards for global positioning system/aircraft based augmentation system airborne equipment) appendix R, tightly integrated GPS/Inertial systems shall meet the FDE requirements summarized in Table1, these requirements are adopted for the tightly integrated BDS/SINS implementation.

Parameter	Requirement
Missed alert probability (satellite failure)	0.001
False alert rate	10 ⁻⁵ / <i>hr</i>
Probability (P _{mi}) of exceeding HPL _{FD}	10 ⁻⁷ / <i>hr</i>
Probability(Pmi)of exceeding HPLFF	10 ⁻⁵ / <i>hr</i>
Failed exclusion probability (satellite failure)	0.001

Table 1 Summary of FDE requirements[6]

2. Tightly integrated BDS/SINS mechanism

BDS/SINS integrated mechanism have complementary advantages and provide more accurate, reliable and continuous navigation parameters. The BDS receiver measurements limit the error drift of SINS, and SINS improve the continuity and integrity performance of BDS receiver. In order to achieve the required level of integrity, it is necessary to, first, characterize the errors that could impact the user position, and, second, to determine the effect of combined errors at the user level.

BDS receiver error is composed of random errors and biases. Random errors include receiver noise and signal transmission noise, etc. BDS biases include normal tropospheric and ionospheric delays, ionospheric anomalies such as ionospheric storm fronts, multipath errors, satellite clock & ephemeris error, receiver clock error and drift, which are the main sources of pseudo-range error. Tropospheric error can be modeled as a first-order Gauss-Markov process. Ionospheric error can be modeled using the International Reference Ionosphere 2001(IRI-2001) model. It models the ionospheric daily variation, but does not model storms. Significant pseudo-range error caused by ionospheric storm is considered as satellite fault. Normal ionospheric and tropospheric delays can be partially calibrated by dual frequency receiver or certain error models (residual error left), while receiver clock error and drift are estimated during position computation [3].

SINS errors are mainly IMU sensor errors, alignment error, and computation error [4]. Sensor errors include dead zone errors, random drift errors, and scale factor errors of gyroscope and accelerometer. Alignment errors are caused by the difference between the real aircraft position and the entered alignment position, or position error from the last updated computation of Kalman filter in integrated system. The computation error mainly includes the quantization error, cumulative error and earth reference ellipsoid parameter errors.

2.1 Error Models

BDS/SINS integrated navigation system use Kalman filters to integrate inertial information with BDS measurements. The Kalman filter relies on an accurate inertial error model and known statistical inertial sensor error distributions as well as a linearized measurement model for BDS pseudo-ranges and the associated pseudo-range error statistics. The BDS/SINS integrated navigation system errors can be divided into six categories according to their characteristics [3~5].

2.1.1 Step Error

Step error is sudden occurred constant error lasts for a period of time and then disappears, which can be expressed as:

$$f(t) = Au(t - t_0) \tag{1}$$

Where A is the amplitude of the error, $u(t-t_0)$ is unit step function with starting time t_0 . When the error is large, it is easy to be detected using snapshot integrity monitoring algorithm. Some of the navigation errors can be considered as step errors, such as faulty satellite, ionospheric storm, receiver delay lock loop (DLL) discriminator track the wrong peak, etc.

2.1.2 Ramp Error

Ramp error is a kind of error that gradually changing with time changing, which can be expressed as:

$$f(t) = R(t - t_0)u(t - t_0)$$
(2)

Where R is the ramp, $u(t-t_0)$ is unit step function with starting time t_0 . Most BDS and SINS errors can be expressed as a ramp error with different ramp or superposition of a cluster of ramp errors. Ramp error with small slope can only be detected when the error accumulates to a certain extent. A sudden frequency shift in the satellite clock will lead to a ramp in the pseudo range, equipment aging, ionospheric storm fronts may also cause such kind of errors.

2.1.3 Random Noise

Receiver noise, gyro/accelerometer noise are all random noise, which can be expressed as:

$$f(t) = A_k u(t - t_0), \quad Ak = \begin{cases} N(0, \sum k), k < t_0 \\ N(\eta(k, t_0), \sum k), k \ge t_0 \end{cases}$$
(3)

Where N(m, V) is Gaussian normal distribution, m is mean, V is covariance, η is mean error, $u(t-t_0)$ is unit step function with starting time t_0 .

2.1.4 First-order Gauss-Markov process

Satellite clock & ephemeris error, gyroscope & accelerometer errors can be modeled as first-order Gauss-Markov process. No correlation is assumed between satellites and different inertial sensors. A first-order Gauss-Markov process can be expressed as:

$$\dot{\mathbf{x}}(\mathbf{t}) = -\beta \mathbf{x}(\mathbf{t}) + \omega(\mathbf{t}) \tag{4}$$

Where β is the correlation time, $\omega(t)$ is random noise.

2.1.5 Oscillation error

Due to the SINS horizontal Schuler coupling and other long term coupling effects, the inertial position error growth has an 84.4minute oscillatory component, and the residuals often gradually deviate from zero in an oscillatory manner. Oscillation error can be expressed as:

$$f(t) = A\sin(t - \theta)u(t - t_0)$$
 (5)

where A is the amplitude of the error, θ is the phase.

2.2 Tightly integrated BDS/SINS using Kalman filter

The tightly integrated BDS/SINS navigation system mechanism shown in figure1 integrate the pseudo-range measurements (pseudo-range, pseudo-range rate) from the BDS receiver and the SINS outputs to get more accurate navigation parameters [7,8]. Kalman filter is used in this paper, equations of pseudo-range and pseudo-range rate in relation with SINS position and velocity is used as measurement equation after linearization.

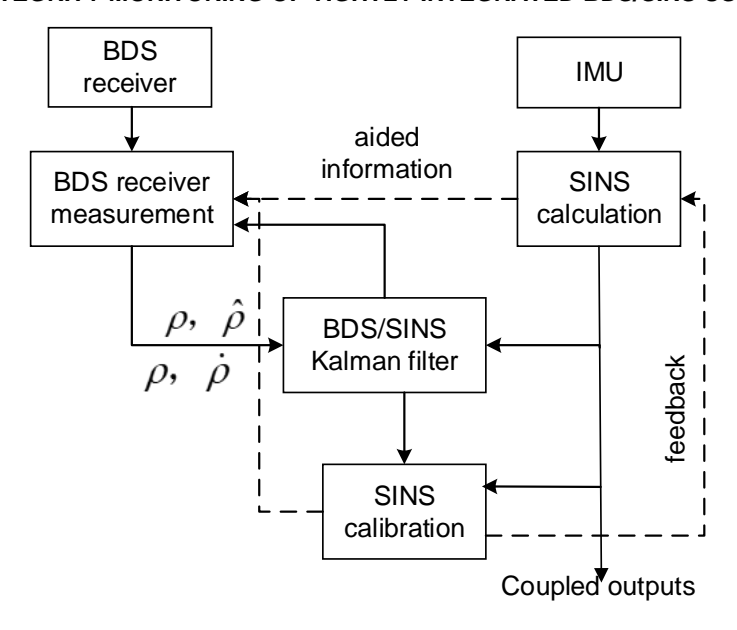


Figure 1 – Tightly integrated BDS/SINS

2.2.1 State vector equation

In tightly integrated BDS/SINS, the system state vector equation of Kalman filter includes the error equation of SINS and BDS. The state vector equations of SINS are expressed in the earth center earth fixed (ECEF) coordinate. The state vector includes position errors, velocity errors, attitude and heading errors, and accelerometer and gyro errors.

$$\mathbf{X}_{l}(t) = \left[\delta r_{x}, \delta r_{y}, \delta r_{z}, \delta v_{x}, \delta v_{y}, \delta v_{z}, \delta \varphi_{x}, \delta \varphi_{y}, \delta \varphi_{z}, b_{gx}, b_{gy}, b_{gz}, b_{ax}, b_{ay}, b_{az}\right]^{T}$$

where the subscripts x, y and z represent the three axes in the ECEF coordinate, δr_x , δr_y and δr_z are the position errors, δv_x , δv_y and δv_z are the velocity errors, $\delta \varphi_x$ and $\delta \varphi_y$ are the attitude errors, $\delta \varphi_z$ is heading error, b_{gx} , b_{gy} and b_{gz} are the gyroscope constant drift, b_{ax} , b_{ay} and b_{az} are the accelerometer constant drift, w_{gx} , w_{gy} and w_{gz} are gyroscope random noise, w_{ax} , w_{ay} and w_{az} are accelerometer random noises. Hence, the SINS state vector equation is as follows [6~8]:

$$\dot{\mathbf{X}}_{I}(t) = \mathbf{F}_{I}(t)\mathbf{X}_{I}(t) + \mathbf{G}_{I}(t)\mathbf{W}_{I}(t)$$
(6)

The state transition matrix is as follows:

$$\mathbf{F}_{I}(t) = \begin{bmatrix} \mathbf{0}_{3} & \mathbf{I}_{3} & \mathbf{0}_{3} & \mathbf{0}_{3} & \mathbf{0}_{3} \\ \mathbf{F}_{21} & -2\mathbf{\Omega}_{ie}^{e} & \mathbf{F}_{23} & \mathbf{0}_{3} & \mathbf{C}_{b}^{n} \\ \mathbf{0}_{3} & \mathbf{0}_{3} & -\mathbf{\Omega}_{ie}^{e} & \mathbf{C}_{b}^{n} & \mathbf{0}_{3} \\ \mathbf{0}_{3} & \mathbf{0}_{3} & \mathbf{0}_{3} & \mathbf{0}_{3} & \mathbf{0}_{3} \\ \mathbf{0}_{3} & \mathbf{0}_{3} & \mathbf{0}_{3} & \mathbf{0}_{3} & \mathbf{0}_{3} \end{bmatrix}$$

The nonzero parts of this matrix is:

 $\mathbf{F}_{21} = -\frac{2\mathbf{\gamma}_{ib}^e}{r_{eS}^e} \frac{r_{eb}^{eT}}{\left|r_{eb}^e\right|}$, $\mathbf{\gamma}_{ib}^e$ is gravitational acceleration in the ECEF coordinate. While r_{eS}^e is the reference ellipsoid radius.

$$\mathbf{F}_{23} = \begin{bmatrix} 0 & f_{ib,z}^{e} & -f_{ib,y}^{e} \\ -f_{ib,z}^{e} & 0 & f_{ib,x}^{e} \\ f_{ib,y}^{e} & -f_{ib,x}^{e} & 0 \end{bmatrix}$$

$$W_B(t) = \begin{bmatrix} w_{gx} & w_{gy} & w_{gz} & w_{ax} & w_{ay} & w_{az} \end{bmatrix}^T$$

$$G_{B}(t) = I_{6\times6}$$

Two BDS receiver clock related errors are listed in the state vectors, one is the equivalent range error caused by the receiver clock error (expressed as δt_u) and the other is the equivalent range rate error caused by the receiver clock frequency error (expressed as δt_{ru}). The latter is a first-order Markov process. The differential equations of these two states are:

$$\begin{cases} \delta \dot{t}_{u} = \delta t_{u} + W_{tu} \\ \delta \dot{t}_{ru} = -\beta_{tru} \delta t_{ru} + W_{tru} \end{cases}$$
 (7)

Where β_{tru} is the correlation time, w_{tu} and w_{tru} are white noise[9,10].

Therefore, the state vector equation of the BDS receiver is:

$$\dot{\mathbf{X}}_{R}(t) = \mathbf{F}_{R}(t)\mathbf{X}_{R}(t) + \mathbf{G}_{R}(t)\mathbf{W}_{R}(t) \tag{8}$$

Where,

$$\mathbf{X}_{B}(t) = \begin{bmatrix} \delta t_{u} \\ \delta t_{ru} \end{bmatrix} \quad \mathbf{F}_{B}(t) = \begin{bmatrix} 0 & 0 \\ 1 & 0 \end{bmatrix} \quad W_{B}(t) = \begin{bmatrix} w_{tu} \\ w_{tru} \end{bmatrix} \quad G_{B}(t) = \begin{bmatrix} 1 & 0 \\ 0 & 1 \end{bmatrix}$$

The state vector equation of tightly integrated BDS/SINS system for Kalman filter can be obtained by combination of equation (6) and equation (8):

$$\begin{bmatrix} \dot{\mathbf{X}}_{I}(t) \\ \dot{\mathbf{X}}_{B}(t) \end{bmatrix} = \begin{bmatrix} \mathbf{F}_{I}(t) & 0 \\ 0 & \mathbf{F}_{B}(t) \end{bmatrix} \begin{bmatrix} \mathbf{X}_{I}(t) \\ \mathbf{X}_{B}(t) \end{bmatrix} + \begin{bmatrix} \mathbf{G}_{I}(t) & 0 \\ 0 & \mathbf{G}_{B}(t) \end{bmatrix} \begin{bmatrix} \mathbf{W}_{I}(t) \\ \mathbf{W}_{B}(t) \end{bmatrix}$$
(9)

that is:

$$\dot{\mathbf{X}}(t) = \mathbf{F}(t)\mathbf{X}(t) + \mathbf{G}(t)\mathbf{W}(t) \tag{10}$$

where.

$$\mathbf{X}(t) = \left[\delta r_{x}, \delta r_{y}, \delta r_{z}, \delta v_{x}, \delta v_{y}, \delta v_{z}, \delta \varphi_{x}, \delta \varphi_{y}, \delta \varphi_{z}, b_{gx}, b_{gy}, b_{gz}, b_{ax}, b_{ay}, b_{az}, \delta t_{u}, \delta t_{ru}\right]^{T}$$

2.2.2 Measurement equation

Assuming that the SINS position of the aircraft and the *i*th satellite position are (x_i, y_i, z_i) and (x_{si}, y_{si}, z_{si}) respectively in the ECEF coordinates, the range between the SINS computed position and the *i*th satellite (inertial pseudo-range) is as follows:

$$\rho_{li} = \sqrt{(X_l - X_{si})^2 + (y_l - y_{si})^2 + (Z_l - Z_{si})^2}$$
(11)

Equation (11) then be linearized as:

$$\rho_{li} = \sqrt{(\mathbf{X} - \mathbf{X}_{si})^2 + (\mathbf{y} - \mathbf{y}_{si})^2 + (\mathbf{Z} - \mathbf{Z}_{si})^2} + \frac{\partial \rho_{li}}{\partial \mathbf{X}_{li}} \delta \mathbf{X} + \frac{\partial \rho_{li}}{\partial \mathbf{y}_{li}} \delta \mathbf{y} + \frac{\partial \rho_{li}}{\partial \mathbf{Z}_{li}} \delta \mathbf{Z}$$
(12)

Where:

$$\frac{\partial \rho_{li}}{\partial X_{li}} = \frac{X - X_{si}}{\sqrt{(X - X_{si})^2 + (Y - Y_{si})^2 + (Z - Z_{si})^2}} = \frac{X - X_{si}}{r_i} = e_{i1}$$

$$\frac{\partial \rho_{li}}{\partial y_{li}} = \frac{y - y_{si}}{\sqrt{(x - x_{si})^2 + (y - y_{si})^2 + (z - z_{si})^2}} = \frac{y - y_{si}}{r_i} = e_{i2}$$

$$\frac{\partial \rho_{li}}{\partial Z_{li}} = \frac{Z - Z_{si}}{\sqrt{(x - X_{si})^2 + (y - Y_{si})^2 + (z - Z_{si})^2}} = \frac{Z - Z_{si}}{r_i} = e_{i3}$$

The inertial pseudo-range is then expressed as:

$$\rho_{ii} = r_i + e_{i1}\delta X + e_{i2}\delta Y + e_{i3}\delta Z \tag{13}$$

The BDS receiver measured pseudo-range of the *i*th satellite is $\rho_{Bi} = r_i - \delta t_u - v_\rho$, where δt_u is the equivalent range error caused by the receiver clock error, and v_ρ is the measurement noise, which is caused by the pseudo-range residual of the multipath error, tropospheric and ionospheric correction residual, etc.

Assume the number of satellites insight is *m*, the measurement equation is as follows:

$$\mathbf{Z}_{\rho} = \begin{bmatrix} \rho_{I1} - \rho_{B1} \\ \rho_{I2} - \rho_{B2} \\ \vdots \\ \rho_{Im} - \rho_{Bm} \end{bmatrix} = \begin{bmatrix} \mathbf{e}_{11} & \mathbf{e}_{12} & \mathbf{e}_{13} & 1 \\ \mathbf{e}_{21} & \mathbf{e}_{23} & \mathbf{e}_{23} & 1 \\ \vdots & \vdots & \vdots & \vdots \\ \mathbf{e}_{m1} & \mathbf{e}_{m2} & \mathbf{e}_{m3} & 1 \end{bmatrix} \begin{bmatrix} \delta \mathbf{x} \\ \delta \mathbf{y} \\ \delta \mathbf{z} \\ \delta \mathbf{t}_{u} \end{bmatrix} + \begin{bmatrix} \mathbf{v}_{\rho 1} \\ \mathbf{v}_{\rho 2} \\ \vdots \\ \mathbf{v}_{\rho m} \end{bmatrix}$$
(14)

Which can be expressed as:

$$\mathbf{Z}_{\rho}(t) = \mathbf{H}_{\rho}(t)\mathbf{X}(t) + \mathbf{V}_{\rho}(t) \tag{15}$$

 $\text{ where } \mathbf{H}_{\!\scriptscriptstyle\rho}(t)\!\!=\!\!\begin{bmatrix}\mathbf{h}_{\scriptscriptstyle\rho1} & \mathbf{0}_{\scriptscriptstyle m\!\times\!12} & \mathbf{h}_{\scriptscriptstyle\rho2} & \mathbf{0}_{\scriptscriptstyle m\!\times\!1}\end{bmatrix}\!,$

$$\mathbf{h}_{\rho 1} = \begin{bmatrix} \mathbf{e}_{11} & \mathbf{e}_{12} & \mathbf{e}_{13} \\ \mathbf{e}_{21} & \mathbf{e}_{23} & \mathbf{e}_{23} \\ \vdots & \vdots & \vdots \\ \mathbf{e}_{m1} & \mathbf{e}_{m2} & \mathbf{e}_{m3} \end{bmatrix} \quad \mathbf{h}_{\rho 2} = \begin{bmatrix} \mathbf{1} \\ \mathbf{1} \\ \vdots \\ \mathbf{1} \end{bmatrix} \quad V_{\rho}(t) = \begin{bmatrix} V_{\rho 1} \\ V_{\rho 2} \\ \vdots \\ V_{\rho m} \end{bmatrix}$$
(16)

In the same way, linearize the range rate error between SINS velocity and the ith satellite:

$$\dot{\rho}_{li} = \dot{r}_{l} + e_{l1}(\dot{x}_{l} - \dot{x}_{si}) + e_{l2}(\dot{y}_{l} - \dot{y}_{si}) + e_{l3}(\dot{z}_{l} - \dot{z}_{si}) \tag{17}$$

$$\dot{\rho}_{i} = \frac{(x - x_{si})(\dot{x} - \dot{x}_{si}) + (y - y_{si})(\dot{y} - \dot{y}_{si}) + (z - z_{si})(\dot{z} - \dot{z}_{si})}{\sqrt{(x - x_{si})^{2} + (y - y_{si})^{2} + (z - z_{si})^{2}}}$$

$$= e_{i1}(\dot{x} - \dot{x}_{si}) + e_{i2}(\dot{y} - \dot{y}_{si}) + e_{i3}(\dot{z} - \dot{z}_{si})$$
(18)

Thus, the range rate of SINS can be expressed as:

$$\dot{\rho}_{li} = \dot{r}_i + \mathbf{e}_{i1} \delta \dot{\mathbf{x}} + \mathbf{e}_{i2} \delta \dot{\mathbf{y}} + \mathbf{e}_{i3} \delta \dot{\mathbf{z}}$$
(19)

While the pseudo-range rate measured by the BDS receiver is:

$$\dot{\rho}_{Bi} = \dot{r}_i - \delta t_{ru} - V_{\dot{\rho}} \tag{20}$$

The pseudo-range rate measurement equation of the tightly integrated BDS/SINS system is as follows according to equation (19) and (21):

$$\mathbf{Z}_{\dot{\rho}} = \begin{bmatrix} \dot{\rho}_{I1} - \dot{\rho}_{B1} \\ \dot{\rho}_{I2} - \dot{\rho}_{B2} \\ \vdots \\ \dot{\rho}_{Im} - \dot{\rho}_{Bm} \end{bmatrix} = \begin{bmatrix} \mathbf{e}_{11} & \mathbf{e}_{12} & \mathbf{e}_{13} & 1 \\ \mathbf{e}_{21} & \mathbf{e}_{23} & \mathbf{e}_{23} & 1 \\ \vdots & \vdots & \vdots & \vdots \\ \mathbf{e}_{m1} & \mathbf{e}_{m2} & \mathbf{e}_{m3} & 1 \end{bmatrix} \begin{bmatrix} \delta \mathbf{v}_{x} \\ \delta \mathbf{v}_{y} \\ \delta \mathbf{v}_{z} \\ \delta \mathbf{t}_{nu} \end{bmatrix} + \begin{bmatrix} \mathbf{v}_{\dot{\rho}1} \\ \mathbf{v}_{\dot{\rho}2} \\ \vdots \\ \mathbf{v}_{\dot{\rho}m} \end{bmatrix}$$
(21)

Thus, the pseudo-range rate measurement equation of Kalman filter can be expressed as:

$$\mathbf{Z}_{\dot{\rho}}(t) = \mathbf{H}_{\dot{\rho}}(t)\mathbf{X}(t) + \mathbf{V}_{\dot{\rho}}(t)
\mathbf{H}_{\dot{\rho}}(t) = \begin{bmatrix} \mathbf{0}_{m \times 3} & \mathbf{h}_{\dot{\rho}1} & \mathbf{0}_{m \times 10} & \mathbf{h}_{\dot{\rho}2} \end{bmatrix}
\mathbf{h}_{\dot{\rho}1} = \begin{bmatrix} \mathbf{e}_{11} & \mathbf{e}_{12} & \mathbf{e}_{13} \\ \mathbf{e}_{21} & \mathbf{e}_{23} & \mathbf{e}_{23} \\ \vdots & \vdots & \vdots \\ \mathbf{e}_{m4} & \mathbf{e}_{m9} & \mathbf{e}_{m9} \end{bmatrix} \quad \mathbf{h}_{\dot{\rho}2} = \begin{bmatrix} 1 \\ 1 \\ \vdots \\ 1 \end{bmatrix} \quad \mathbf{V}_{\dot{\rho}}(t) = \begin{bmatrix} \mathbf{V}_{\dot{\rho}1} \\ \mathbf{V}_{\dot{\rho}2} \\ \vdots \\ \mathbf{V}_{\dot{\rho}m} \end{bmatrix}$$

So we get the measurement equation of pseudo-range and pseudo-range rate as follows:

$$\begin{bmatrix} \mathbf{Z}_{\rho} \\ \mathbf{Z}_{\dot{\rho}} \end{bmatrix} = \begin{bmatrix} \mathbf{H}_{\rho} \\ \mathbf{H}_{\dot{\rho}} \end{bmatrix} \mathbf{X} + \begin{bmatrix} \mathbf{V}_{\rho} \\ \mathbf{V}_{\dot{\rho}} \end{bmatrix}$$
 (23)

3. Integrity monitoring based on MHSS

Commercial aircraft usually equipped with two or three sets of SINS. The SINS outputs are compared before integration, and the faulty equipment will be isolated from being used for integration. Considering the airworthiness requirement of the airborne SINS and inertial sensors redundancy, SINS fault is ignored in the BDS/SINS tight coupled navigation, and the integrity monitoring function focuses on faulty satellite detection and exclusion. For precise positioning, satellites with significant pseudo-ranging errors are considered as faulty satellites and should be exclude from navigation computation, which means multiple satellites fault condition should be considered. Multiple Kalman filters are chosen to manage this, by excluding a different satellite in each filter, the residual and additional bias states are used for fault exclusion.

There are several methods for FDE, such as pre-residual (Innovation) Screening, post-residual monitoring, extrapolation method, etc. [9,10] The pre-residual (Innovation) Screening and post-residual monitoring method provide fault exclusion capability for large steps, ramps and ramp rates, but not work well on slow drifts or drift rates fault exclusion. The extrapolation method utilizes a simultaneous combination of both transient and redundancy effects to detect failures, which stores over 30 minute periods' measurements in buffers, provides detection capability for slow failures because of the information that is retained from previously processed measurements. Massive measurements data stored occupies computer resources. For conventional Kalman filter, when redundant satellite information is available, errors will develop in all satellite post residuals or pre residuals as a satellite failure progresses and the initial transient has settled. FDE method solely based on remaining residuals is approximately equivalent to traditional RAIM function and not further augment the integrity monitoring.

Solution separation method use a bank of Kalman filters provides a non-transient fault detection and exclusion capability based on the redundancy information retained from previously processed measurements via the inertial function, HPL computation is an integral part of this method. The enhancement provided by external aiding information, such as receiver clock, is incorporated in the calculated HPL. No miss-calibration is possible since one of the reference sub-filters using the aiding will not contain the failing satellite.

According to the required navigation performance (RNP) concept, Time to Alert (TTA) is the maximum allowable elapsed time from the onset of a positioning failure until the equipment annunciates the alert, any data that is output to other equipment or displayed to the pilot that has an error larger than the horizontal alert limit (HAL) or current horizontal protection level (HPL), without an indication of the warning within the TTA for the applicable phase of flight will cause integrity risk, as specified in table1.

3.1 Multi-hypnosis Solution Separation with Kalman filter

Figure 2 is the structure of Kalman filter with solution separation, which includes one main filter F_{00} ,

N sub-filters of F_{01} - F_{0N} and N-1 secondary sub-filters for each sub-filter. The main filter contains measurement vectors of all satellite in view, the sub-filter F_{0N} contains the measurements of N-1 satellites in view except the Nth satellite, and the secondary sub-filter F_{NM} contains the measurements of N-2 satellites in view except the Nth and Mth satellite. SINS data are used in all filters (main and sub- filters) with no exceptions. Significant deviation occurs between at least one sub-filter and the main filter when there is a faulty satellite. Compare the filter output deviation with the threshold, the integrated system will give out alert and isolate the faulty satellite according to the separation solution of the sub-filter and the secondary sub-filter[11,12].

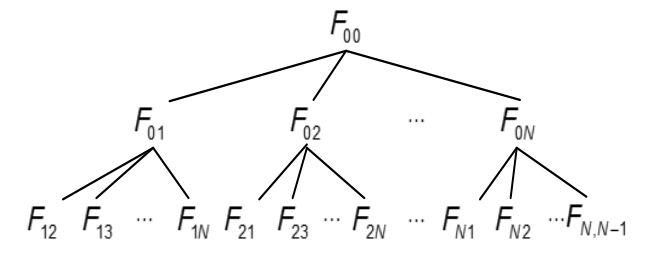


Figure 2 - Solution separation Kalman filter

3.2 Integrity monitoring based on multi-solution separation

The separation vector of the estimated solutions between the main filter and one of the sub-filter at time k is as follows:

$$\mathbf{dX}_{0nk} = \hat{\mathbf{X}}_{0nk} - \hat{\mathbf{X}}_{0nk} \quad n = 1, \dots, N$$
 (24)

Its covariance is:

$$\alpha \mathbf{P}_{0n,k} = E\left(\alpha \mathbf{X}_{0n,k} \cdot \alpha \mathbf{X}_{0n,k}^{T}\right) = \mathbf{P}_{00,k} - \mathbf{P}_{0n,k}^{cross} - \left(\mathbf{P}_{0n,k}^{cross}\right)^{T} + \mathbf{P}_{0n,k}$$
(25)

Where $\hat{\mathbf{\chi}}_{0n,k}$ is the state vector of Kalman filter for BDS/SINS integrated system, \mathbf{P}_{00} , \mathbf{P}_{0n} and \mathbf{P}_{0n}^{cross} are the covariance matrix of corresponding estimated solution separation vectors respectively [12]. The test statistics for each sub-filter is:

$$d_{0n} = \sqrt{\left(d\mathbf{X}_{0n}[1]\right)^2 + \left(d\mathbf{X}_{0n}[2]\right)^2}$$
 (26)

The decision threshold T_{0n} of each sub-filter is obtained according to the required false alert rate P_{FA} :

$$T_{0n} = \sqrt{\lambda^{dP}} \operatorname{erf}^{-1} (1 - P_{FA} / (2N))$$
 (27)

Where λ^{dP} is the maximum eigenvalue of $d\mathbf{P}_{0n}^{\text{hpos}}$, which means the covariance in the direction of maximum error[11,13].

Fault detection and exclusion is done according to the test statistics of the N sub-filter's outputs. The criteria are as follows:

- (1) Fault free H_0 : Test statistics of all the sub-filters are $d_{0n} \le T_{0n}$
- (2) Faulty condition H_1 : exit at least one sub-filter's test statistics $d_{0n} > T_{0n}$.

Fault isolation can be achieved using the solution separation of sub-filters and their secondary sub-filters. Similar to fault detection methods, satellite r is confirmed fault using the test statistics d_{nm} and decision threshold T_{nm} according to the following criteria: For all $n \neq r$ satellites, there is at least one test statistic of the filter that exceeds the decision threshold, i.e. $d_{nm} > T_{nm}$, and for all $r \neq m$, $d_m \leq T_{rm}$ [11,13].

As the tightly integrated BDS/SINS system can propagate the established position accurately if the BDS signals are lost due to any unexpected event such as interference, scintillation, masking, unexpected satellite failure, etc. integrity coasting should be considered. The horizontal protection level (HPL) calculation take into account the mis-calibration of the hybrid solution due to the undetected failure. The horizontal protection level for each sub-filter is calculated as follows:

$$HPL_n = T_{0n} + a_{0n} \tag{28}$$

Where T_{0n} is the decision threshold corresponding to the sub-filter, and a_{0n} is the horizontal position error threshold of sub-filter F_{0n} . a_{0n} is calculated according to the missing detection rate P_{MD} :

$$a_{0n} = \sqrt{\lambda^{P_{0n}}} \operatorname{erf}^{-1} (1 - P_{MD})$$
 (29)

 $\lambda^{P_{0n}}$ is the maximum eigenvalue of the horizontal position error vector covariance matrix \mathbf{P}_{0n} .

The horizontal protection level of the integrated BDS/SINS system is as follows.

$$HPL=\max(HPL_n)=\max(T_{0n}+a_{0n})$$
(30)

4. Monte Carlo verification of system integrity monitoring

To verify the performance of the algorithm, simulation is implemented using the following parameters: The three accelerometers biases are set as $30\mu g$, - $45\mu g$ and $26\mu g$, the random walk is $20\mu g/\sqrt{hr}$; the initial attitude and heading (pitch, roll and yaw) misalignments are 0.008 deg, -0.01 deg and 0.01 deg respectively. The gyro drifts along the three axis are $9\times10^{-4} deg/hr$, $1.3\times10^{-3} deg/hr$ and $8\times10^{-4} deg/hr$ respectively. Random walk is $0.002 deg/\sqrt{hr}$; SINS output rate is 100 Hz, BDS output rate is 1Hz, false alert rate P_{FA} is 0.333×10^{-6} , and missed detection rate P_{MA} is 0.001.

The BDS receiver chooses visible satellites with the largest GDOP in each available space-time point for navigation calculation [14]. Pseudo-range errors are added to the most difficult detectable satellite to simulate satellite fault. Assuming GEO3 satellite has a ramp of 0.63 m/s at 11s, which lasting 129 seconds. The flight phase is set as terminal non-precision approach, with the requirements of missed alert, false alert probability and TTA limit defined for non-precision approach.

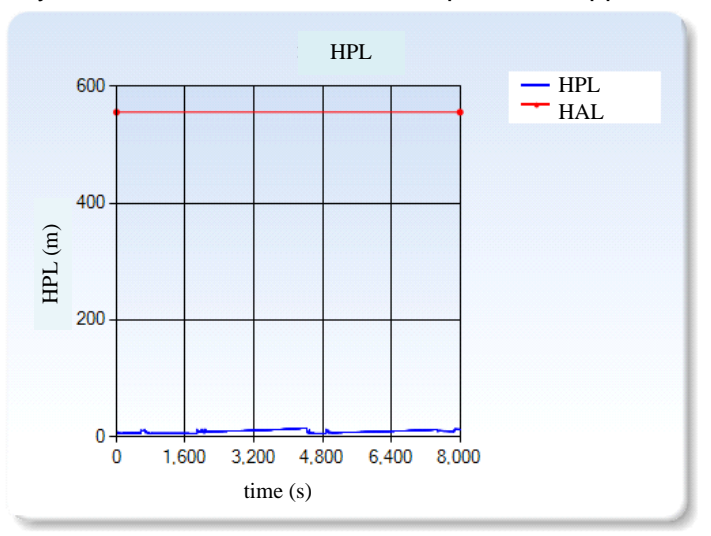
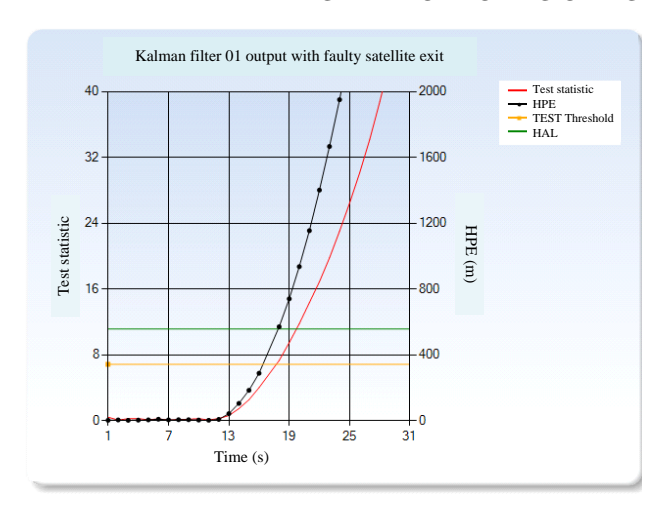
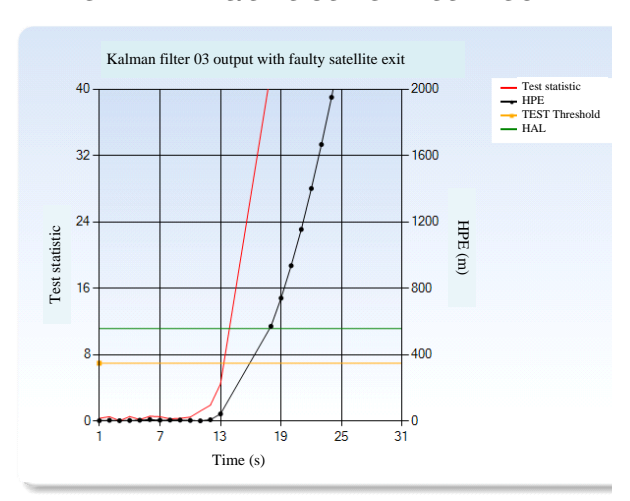


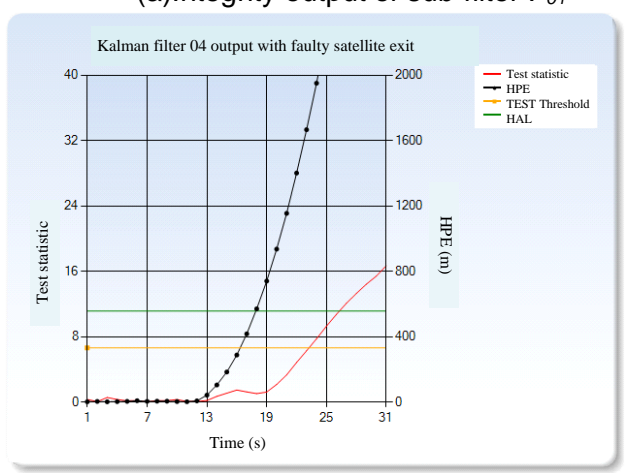
Figure 3 – HPL using solution separation algorithm

The outputs of each Kalman filter are shown in figure 4 when the fault occurs, where we can find that, the test statistics of the sub-filter F_{03} exceed the detection threshold and an alert occurs at 13s. The horizontal positioning errors of the sub-filters exceed the horizontal alert limit at 18s. The simulation results showed that: the solution separation method can detect and exclude fault satellite with slowly ramp and the fault alert is given out in time (not exceed TTA limit).

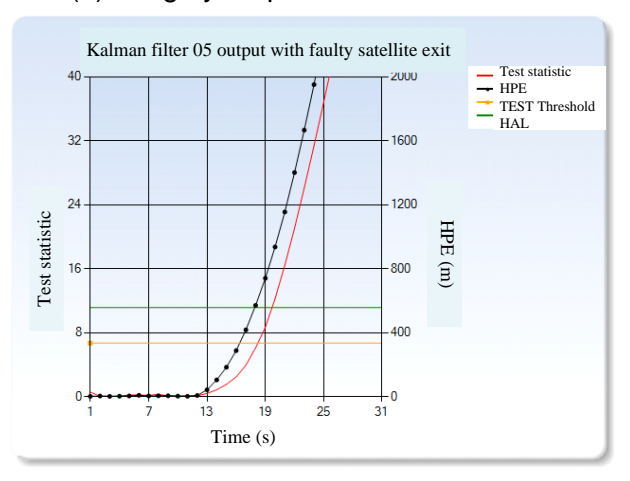




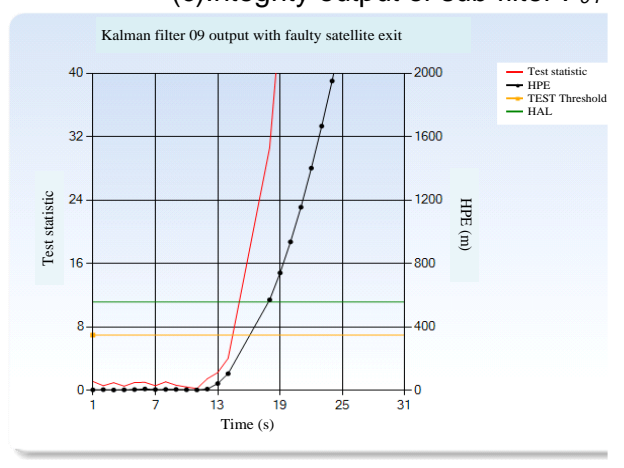
(a)Integrity output of sub-filter F_{01}



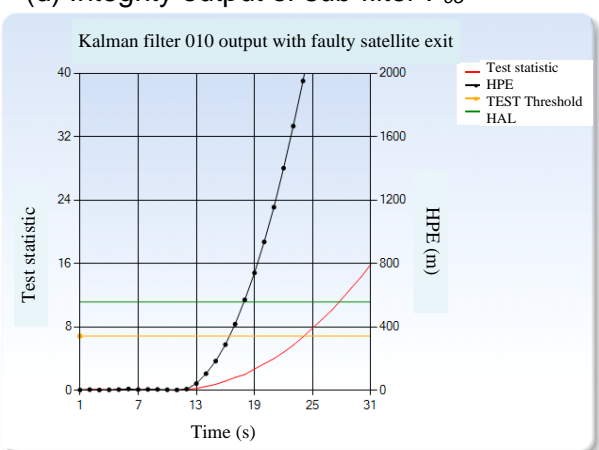
(b) Integrity output of sub-filter F_{02}



(c)Integrity output of sub-filter F₀₄



(d) Integrity output of sub-filter F_{05}



(e)Integrity output of sub-filter F₀₉

(f) Integrity output of sub-filter F_{010}

Figure 4 – Integrity outputs of sub-filters when faulty satellite exit

Monte Carlo simulation is implemented to verify the false alert rate and the missed detection rate of the algorithm. 8000 Monte Carlo simulations with randomly generated faults in every 120 seconds are used. The test results are shown in figure5, and the statistical result are listed in Table2.

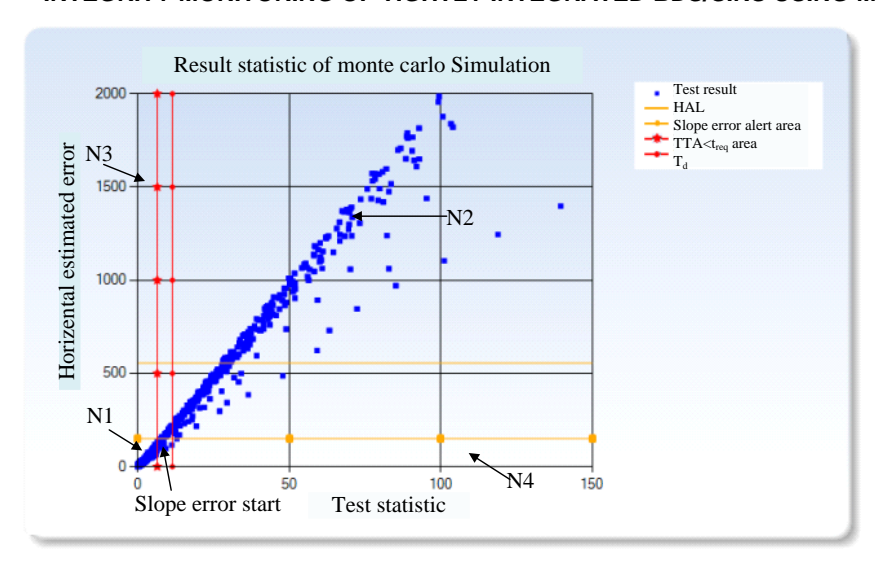


Figure 5 – Monte Carlo simulation result

Table2 statistical result of Monte Carlo simulation

Item	normal (N_1)	Detected in time (N_2)	missed detection (N ₃)	False alert (N ₄)
Number	7049	770	0	1

According to the statistical results, the false alert rate is 1.25×10⁻⁴ (< 1/15000) and the missed detection rate is 0 (<0.001), both parameters meet the requirements. The false alert rate is high because of the solution separation algorithm is sensitive to slow-changing ramp faults.

5. Conclusion

The multi-hypothesis solution separation algorithm is used in tightly integrated BDS/SINS navigation system for integrity monitoring. The error characteristics of SINS and BDS are analyzed first, tightly integrated BDS/SINS mechanism is constructed using Kalman filter, with MHSS algorithm used for integrity monitoring. Six satellites under poor GDOP are selected to verify the system FDE function by artificially added errors to the most hard to be detected satellite, the horizontal protection level is computed at the same time. The simulation results show that this algorithm can effectively realize the FDE function and meet the integrity requirements corresponding flight phase. But this paper only simulated one satellite faulty. When multiple satellites faulty, the same method can be used, but the number of Kalman filters needed will increase dramatically, which will slow down the equipment processing speed.

Acknowledgment

This work was funded by the National Natural Science Foundation of China (U2233215).

Contact Author Email Address

Mailto: sgsun@cauc.edu.cn

Copyright Statement

The authors confirm that they, and/or their company or organization, hold copyright on all of the original material included in this paper. The authors also confirm that they have obtained permission, from the copyright holder of any third party material included in this paper, to publish it as part of their paper. The authors confirm that they give permission, or have obtained permission from the copyright holder of this paper, for the publication and distribution of this paper as part of the ICAS proceedings or as individual off-prints from the proceedings.

References

[1] Blanch J, Walter T. Design of estimators with integrity in the presence of error model uncertainty[C], Proceedings of the 35th International Technical Meeting of the satellite division of the Institute of Navigation (ION GNSS+ 2022), Denver, CO, Vol. 2, pp1435-1448, 2022.

- [2] Blanch J, Walter T. Fast protection levels for fault detection with an application to advanced RAIM[J]. IEEE Transactions on aerospace and electronic systems, Vol. 57, No. 1, pp55-65, 2021.
- [3] Smith A L. An integrated navigation system model for coupled GNSS-inertial navigation research[C]. AAIA modeling and simulation technologies conference, Portland, OR, pp274-286, 2011.
- [4] Jiang D. Integrity monitoring of inertial aided satellite navigation[D], NANJING: Nanjing areospace & aviation university, 2012.
- [5] Bhatti U, Ochieng W. Failure modes and models for integrated GPS/INS system[J]. The Journal of Navigation, Vol. 60, No. 2, pp327-348, 2007.
- [6] RTCA. DO316, Minimum operational performance standards for global positioning system/aircraft based augmentation system airborne equipment [S]. Washington DC: RTCA Inc, April 2009.
- [7] Mohinder S. G, Lawrence R. W and Angus P. A. Global positioning system, inertial navigation and integration, 1st edition, A John Wiley & Son Inc. publication, 2001.
- [8] Li J, BDS/INS integration navigation system fusioning algorithm[D]. Harbin: Harbin engineering university, 2013.
- [9] Hu Z, Performance assesment & experimental verification of BDS[D], Wuhan: Wuhan university, 2013.
- [10]Song M, Tang R, BDS integrity performance test and analysis[J], Beijing Mapping, No. 1, pp109-113, 2015.
- [11]Langel S, Khanafseh S, Chan F, et al. Integrity risk bounding in uncertain linear systems[J]. Journal of Guidance, Control and Dynamics, Vol. 38, No.10, pp1990-1994, 2015.
- [12]Langel S, Khanafseh S, Pervan B. Bounding integrity risk for sequential state estimators with stochastic modeling uncertainty[J]. Journal of Guidance, Control and Dynamics, Vol. 37, No.1, pp36-46, 2014.
- [13]Blanch J, Walter T and Enge P. Theoretical results on the optimal detection statistics for autonomous integrity monitoring[J], Journal of the institute of navigation, Vol. 64, No.1, pp123-137, 2017.
- [14] China Satellite Navigation Offic, BeiDou Navigation Satellite System Open Service Performance Standard (Version 3.0)[S], May, 2021.